

# Can Dynamics Be Responsible for the Complex Multippeak Infrared Spectra of NO Adsorbed to Copper(II) Sites in Zeolites?\*

Florian Göttl,\* Philippe Sautet, and Ive Hermans\*

**Abstract:** Copper-exchanged SSZ-13 is a very efficient material in the selective catalytic reduction of NO<sub>x</sub> using ammonia (deNO<sub>x</sub>-SCR) and characterizing the underlying distribution of copper sites in the material is of prime importance to understand its activity. The IR spectrum of NO adsorbed to divalent copper sites are modeled using *ab initio* molecular dynamics simulations. For most sites, complex multi-peak spectra induced by the thermal motion of the cation as well as the adsorbate are found. A finite temperature spectrum for a specific catalyst was constructed, which shows excellent agreement with previously reported data. Additionally these findings allow active and inactive species in deNO<sub>x</sub>-SCR to be identified. To the best of our knowledge, this is the first time such complex spectra for single molecules adsorbed to single active centers have been reported in heterogeneous catalysis, and we expect similar effects to be important in a large number of systems with mobile active centers.

NO<sub>x</sub> is an undesired byproduct of the combustion of fossil fuels with air, responsible for acid rain. In recent years, ecological awareness has led to more strict legislative emission standards for industrial processes as well as vehicle emissions. Most often, NO<sub>x</sub> is catalytically removed from exhaust gases. This de-NO<sub>x</sub> chemistry is especially challenging for diesel engines, where reaction conditions are compara-

tively harsh. One successful approach is the selective catalytic reduction of NO<sub>x</sub> using NH<sub>3</sub> (deNO<sub>x</sub>-SCR) over transition-metal-exchanged zeolites.<sup>[1–3]</sup> Within this group of materials, copper-exchanged SSZ-13 shows high activity and superior stability over a wide range of operating conditions (such as temperature and humidity).<sup>[4]</sup>

These remarkable properties have not only led to the commercialization of Cu-SSZ-13,<sup>[5]</sup> but also attracted significant scientific interest.<sup>[6,7]</sup> There is a consensus that at low loadings, copper is present as site-isolated ionic species that act as the reactive centers for these reactions.<sup>[6,7]</sup> The reaction pathway has been the subject of discussions.<sup>[8,9]</sup> Most recent work indicates that the nature of the active sites changes in the presence of water, which leads to modified reaction paths for different experimental conditions.<sup>[10]</sup> However, it is well-established that the actual activity of the sites depends on the precise molecular environment of the copper sites, which again depends on the distribution of aluminum centers in the zeolite framework.<sup>[11]</sup>

Characterizing this aluminum distribution is challenging and key to understanding the activity of zeolite catalysts. One of the major influences is the Si/Al ratio. Experimentally SSZ-13 has been synthesized with Si/Al ratios between 4.8<sup>[12]</sup> and 35.<sup>[13]</sup> Most often the ratios are non-integer multiples of single crystallographic unit cells, pointing towards a defect-like behavior of aluminum atoms and the possible presence of more than one aluminum atom in a primitive unit cell. An additional complication stems from the fact that significant amounts of the aluminum are present as ill-defined extra framework aluminum.<sup>[14]</sup> In previous work, some of us suggested four different aluminum distributions for a Si/Al ratio of 6.<sup>[11]</sup> More recent work by Godiksen et al. indicates that already at a Si/Al ratio of 14 five different sites are present.<sup>[15]</sup>

While it is possible to directly address the coordinative environment of aluminum in the material using for example Al-NMR spectroscopy, most characterization methods give indirect information. One of these methods is based on the adsorption of NO to copper(II) sites within the zeolite framework. It has been applied to various zeolite topologies, and recently a very detailed study by Zhang et al. investigated IR spectra of NO adsorbed to copper sites in SSZ-13.<sup>[13]</sup> To deduce statements about the aluminum distribution from such experimental spectra can only be achieved by using electronic structure calculations.<sup>[16]</sup> However, experimental measurements are typically performed at finite temperature, whereas static electronic structure calculations describe the system at 0 K.

Herein we model finite-temperature IR spectra for NO adsorbed on copper(II) sites in SSZ-13 at low Si/Al ratios and

[\*] Dr. F. Göttl, Prof. I. Hermans  
University of Wisconsin-Madison, Department of Chemistry  
1101 University Avenue, 53706 Madison, WI (USA)  
E-mail: fgoettl@chem.wisc.edu  
hermans@chem.wisc.edu

Prof. P. Sautet  
Université de Lyon, CNRS  
Ecole Normale Supérieure de Lyon, Laboratoire de Chimie  
46 Allée d'Italie, F-69342 Lyon Cedex 07 (France)

Prof. I. Hermans  
University of Wisconsin-Madison  
Department of Chemical and Biological Engineering  
1415 Engineering Drive, 53706 Madison, WI (USA)

[\*\*] F.G. and I.H. acknowledge financial support from the University of Wisconsin-Madison and the Wisconsin Alumni Research Foundation (WARF). F.G. acknowledges computational time at the Pôle Scientifique de Modélisation Numérique (PMSN), and National Energy Research Scientific Computing Center (NERSC), a DOE Office of Science User Facility supported by the Office of Science of the U.S. Department of Energy under Project No. m2070-Zeogenome. The authors thank A. Love (UW-Madison) for help with graphical illustration of the article and R. E. Buló (University of Utrecht) for providing an adapted version of the code FlexMD for evaluation of MD trajectories.

Supporting information for this article is available on the WWW under <http://dx.doi.org/10.1002/anie.201501942>.

low copper exchange levels. We find complex multi-peak spectra for all sites. Comparing simulations with published experimental spectra allows the assignment of the copper site distribution. In conjunction with activity data this allows active and inactive sites to be identified for the selective catalytic reduction of  $\text{NO}_x$  using  $\text{NH}_3$ .

SSZ-13 is a zeolite in the chabazite structure. It consists of  $\text{SiO}_4$  and  $\text{AlO}_4$  tetrahedra (T-sites), which share O atoms. The most basic unit cell consists of 12 T-sites, which form a double six-membered oxygen ring structure and these units are connected by four-membered oxygen rings.<sup>[17]</sup> The neutral framework only consists of Si T-sites and the material is activated by substituting Si by Al. This substitution creates a local negative charge, which is neutralized by the presence of a counteranion. There are strong indications that these Al positions are not distributed uniformly, but that, similar to defect sites in metals or metal oxides, it is necessary to consider a distribution of local Al configurations.<sup>[11]</sup> Realistic Si/Al ratios lie between about 5 and 36 and therefore we consider all possible Al distributions in unit cells containing one, two, and three Al atoms (all possibilities are shown in the Supporting Information). To create the divalent  $\text{Cu}^{\text{II}}$  cation we add an OH group to the Cu atom in the one Al unit cell and a proton in the most stable position for the three Al unit cells. In our models, almost all Cu sites are positioned in the six-membered ring. However, to take recent discussions on the exact position of the Cu–OH sites into account,<sup>[18]</sup> we also investigated their position in six- and eight-membered rings.

Typical experimental measurements are performed for macroscopic systems at finite temperatures. One of the key modeling challenges is the inclusion of these effects. Following the ergodic hypothesis we perform *ab initio* molecular dynamics simulations using the Vienna *ab initio* simulation package (VASP).<sup>[19,20]</sup> The sampling time of 75 ps, is a good compromise between ergodicity and computational efficiency. A more detailed discussion is given in the Supporting Information. We calculate finite-temperature IR spectra by Fourier transformation of the distance autocorrelation function.<sup>[21]</sup> To arrive at the measured canonic ensemble and to take the fundamental principles of heat transport in solids into account, we use stochastic boundary conditions as suggested by Kantorovich and Rompotis,<sup>[22]</sup> and use a Langevin thermostat for O-atoms, connecting the double six-membered-ring building blocks. However, to avoid unphysical bias of the spectra, we exclude atoms directly neighboring

Cu atoms or the NO molecule. Furthermore we apply a Gaussian broadening of  $4\text{ cm}^{-1}$ , which corresponds to the experimental resolution.

We studied 11 different sites, and will discuss the four sites displayed in Figure 1 in more detail in the text (all sites and spectra are shown in the Supporting Information). For two of

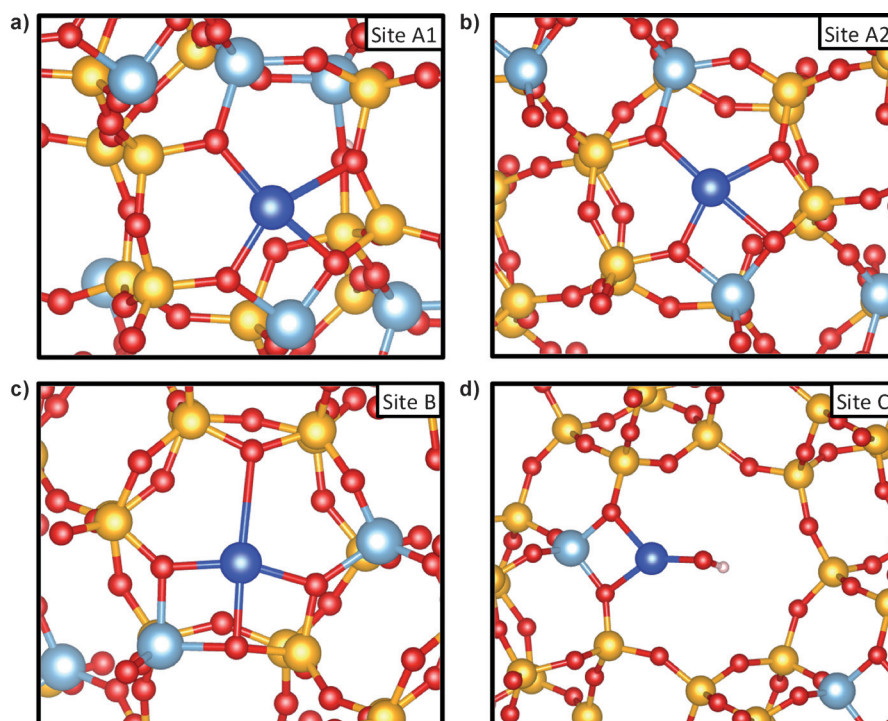


**Figure 1.** The four sites used to construct the finite-temperature IR spectrum of SSZ-13 at low Cu loadings with a Si/Al ratio of 6. The sites differ in the position of the Al-atoms. For sites A1 (a), A2 (b), and B (c), two Al atoms are positioned in the same 6 MR ring. For site C (d), only one Al atom is close to Cu. To arrive at a divalent cation for site A1, a proton is added to an O closest to one Al atom (in (a) it is hidden behind an O). For site C, an OH group is bonded to the Cu atom. O red, Al blue-gray, Cu blue, Si yellow, H white. The remaining 11 calculated sites are given in the Supporting Information.

those sites, the Al atoms are positioned on opposite sides of the same six-membered ring. In one case (site A1, Figure 1a) two Al atoms are present in the unit cell, in the other case (site A2, Figure 1b) three Al atoms are present in the unit cell. For site B (Figure 1c), two Al atoms are positioned in asymmetric position in the same six-membered ring, and site C (Figure 1d) corresponds to one Al atom in the unit cell and a Cu–OH site in the eight-membered ring. The feature of sites A1 and A2 (Figure 2a,b) show a clear two peak spectrum with one peak at  $1900\text{ cm}^{-1}$  and the second peak at about  $1855\text{ cm}^{-1}$  (site A1) and  $1860\text{ cm}^{-1}$  (site A2).<sup>[23]</sup> These spectra are very similar and below we refer to them (if not explicitly mentioned otherwise) as site A. Site B leads to a complex multi-peak spectrum (Figure 2c) with a major peak at about  $1910\text{ cm}^{-1}$ , a shoulder at about  $1895\text{ cm}^{-1}$ , and another peak at  $1860\text{ cm}^{-1}$ . For site C, the signal (Figure 2d) is significantly red-shifted with maxima around  $1780\text{ cm}^{-1}$ . However, the main feature is around  $1840\text{ cm}^{-1}$ . This shift is not surprising, as our molecular dynamics simulations show that the NO

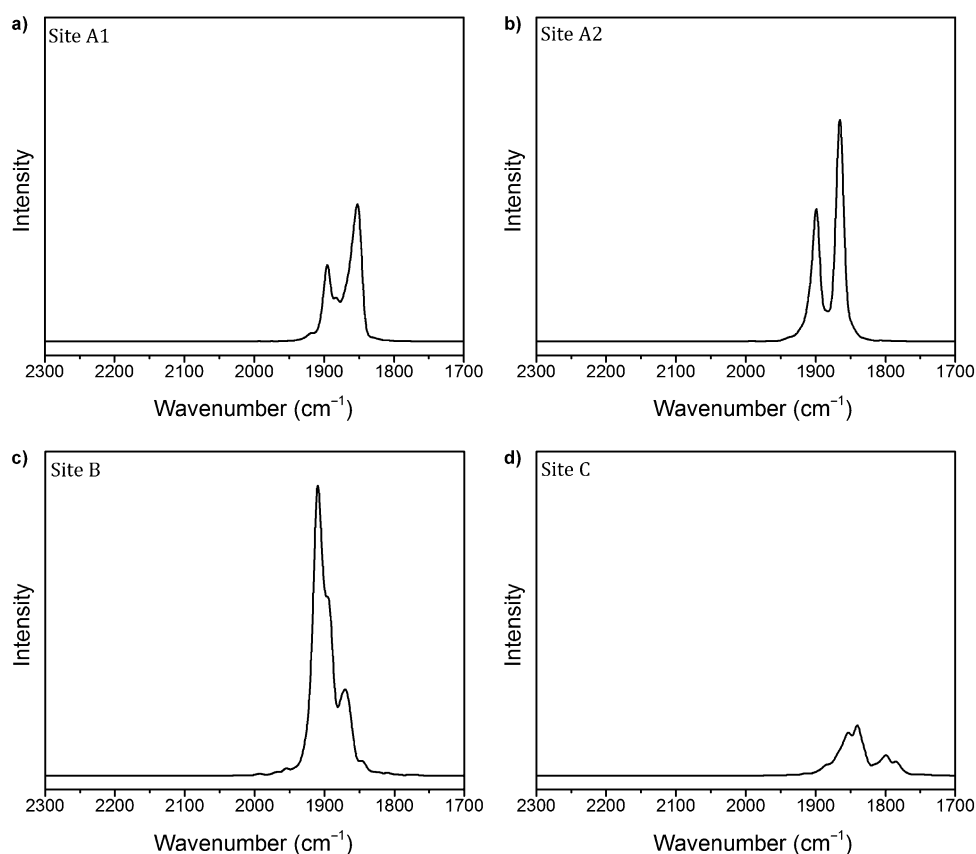


**Figure 2.** At 300 K, all four sites lead to different, complex multi-peak IR spectra. Spectra for a) A1, b) A2, c) B, and d) C.

molecule almost exclusively binds to the O atom of the OH group.

These results clearly show that single active sites in zeolites with a single molecule adsorbed can lead to highly complex multi-peak vibrational spectra. To find the underlying reasons for this behavior, we will analyze sites A2, B, and C in more detail. For site A2,<sup>[25]</sup> finite temperature induces a movement of the Cu atom between two different configurations (see Figure 3), one being in the center of the six-membered ring and bonded to two activated O atoms (configuration I, Figure 3c), while Cu binds to three activated O atoms in the other (configuration II, Figure 3b). We find both configurations as local minima in static calculations, which lead to NO vibrations of  $1866\text{ cm}^{-1}$  for configuration I and  $1912\text{ cm}^{-1}$  for configuration II. These peaks are very similar to the peaks obtained from dynamic calculations and this allows a clear assignment of the spectrum for site A2. When integrating the spectrum up to  $1890\text{ cm}^{-1}$  (see Figure 3a), we find that 62% of the area can be associated with configuration I and 38% with configuration II. At the same time it is possible to analyze the trajectory obtained in our molecular dynamics simulations suggesting that the system is 69% of the time in configuration I and 31% of the time in configuration II. This almost-quantitative agreement corroborates the validity of our assignment.

A more complex situation is encountered for site B, where, additionally to the cation motion, the NO molecule

moves between a configuration bound on top of the Cu atom and lying parallel to the plane of the six-membered ring (shown in the Supporting Information) and two configurations, where it binds to the Cu atom and an O atom on the opposite side of the six-membered ring and is perpendicular to it (shown in the Supporting Information). With the fourth configuration similar to configuration II of site A2, this leads to a total of four different local configurations. It is still possible to perform a trajectory analysis and calculate the corresponding static wavenumber (occupations of 47%, 18%, 13%, and 22% and wavenumbers of  $1906\text{ cm}^{-1}$ ,  $1895\text{ cm}^{-1}$ ,  $1867\text{ cm}^{-1}$  and  $1831\text{ cm}^{-1}$ ). However, the bonding environment of the NO molecule differs greatly for different configurations, which will lead to changes in anharmonic corrections and possibly also a quenching of the NO vibration. Additionally, the differ-

ent small peaks of the spectrum indicate a very flat potential energy surface with many local minima for some of the configurations. In combination with a highly complex structure of the spectrum, this does not allow a simple analysis as for site A2.

For site C, the coordination of Cu does not change significantly. However, in this case the NO molecule does not bind directly to the Cu atom, but to the O of the OH group.<sup>[24]</sup> Therefore it is the orientation of the OH group that has a significant influence on the IR wavenumber. As the OH group is rather mobile, this again leads to highly complex spectra and a clear, quantitative assignment is not possible.

Recently, Zhang et al. published a detailed study on IR spectroscopy of NO adsorbed to Cu sites in SSZ-13.<sup>[13]</sup> In their measurements, they find three different broad bands. The signal between  $2050\text{ cm}^{-1}$  and  $2300\text{ cm}^{-1}$  is assigned to the creation of a  $\text{NO}^+$  species, the band between  $1750\text{ cm}^{-1}$  and  $1850\text{ cm}^{-1}$  to NO adsorbed to  $\text{Cu}^{\text{I}}$  sites,<sup>[26]</sup> and the band between  $1850\text{ cm}^{-1}$  and  $2000\text{ cm}^{-1}$  is assigned to NO adsorbed to  $\text{Cu}^{\text{II}}$ . In the experimental measurements, only small doses of NO were introduced stepwise into the cell per time interval. Thermodynamically speaking, NO initially adsorbs to the most stable adsorption positions, and once those are covered, to the next most stable ones. However, all three signals grow in intensity with each dose. The intensities of these distinct spectroscopic features associated with  $\text{NO}^+$ ,  $\text{Cu}^{\text{II}}\text{-NO}$ , and  $\text{Cu}^{\text{I}}\text{-NO}$  do, however, not increase propor-



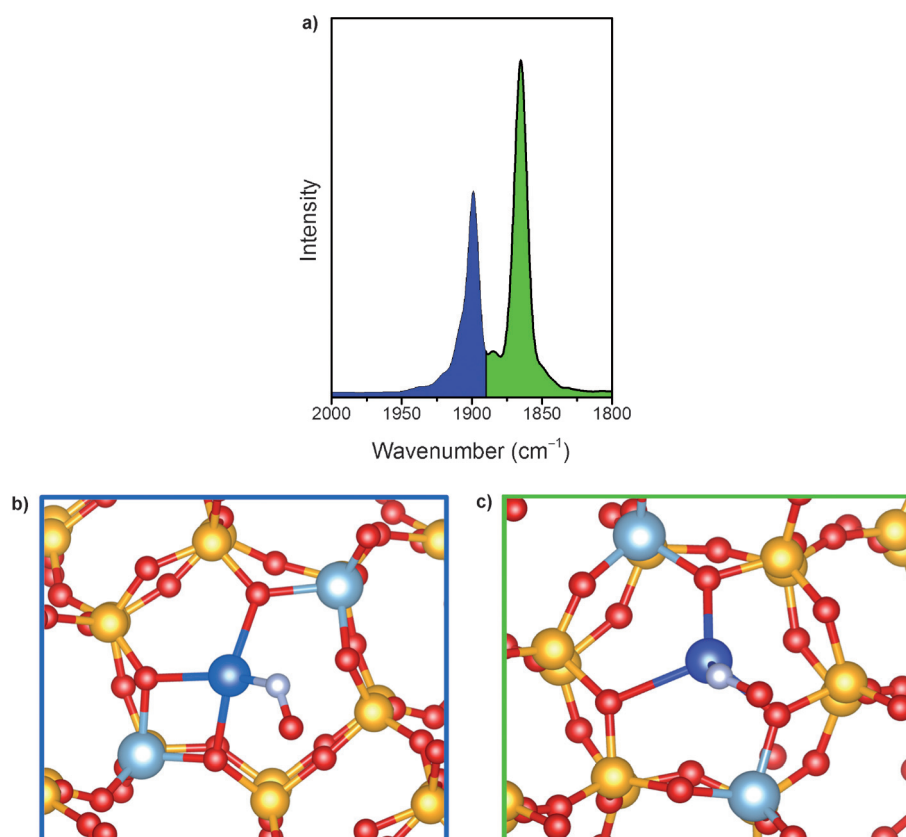


**Figure 3.** Finite temperature leads to complex multi-peak spectra. a) The spectrum for site A. The Cu atom moves between two different coordination configurations displayed in (b) and (c). Upon integrating the area underneath the curve until and above  $1890\text{ cm}^{-1}$  (the green and blue areas), there is excellent agreement with the analysis of the molecular dynamics trajectory. N gray; color code for other atoms is given in Figure 1.

tionally upon consecutive dosages of NO. This strongly suggests that the adsorption preference between different features changes.

In this study we focus on the  $\text{Cu}^{\text{II}}\text{--NO}$  feature (between  $1850\text{ cm}^{-1}$  and  $2000\text{ cm}^{-1}$ ). Owing to the presence of many different local Al distributions, the spectra become highly complex. Therefore we will focus on a sample with  $\text{Si}/\text{Al}=6$  and a very low ion exchange level ( $\text{Cu}/\text{Al}=0.03$ ; the experimental spectrum is displayed in Figure 4a<sup>[13]</sup>), where only the most stable Cu sites will be occupied. To reproduce the experimental spectrum we make the following assumptions (which will be justified below): 1) adsorption of NO to site C is thermodynamically most favorable, followed by adsorption to sites A and B; 2) one sixth of the  $\text{Cu}^{\text{II}}$  sites are of types A and C, while the remaining two thirds are of type B; and 3) for site A, adsorption to the  $\text{Cu}^{\text{II}}$  sites is less favorable compared to the other features ( $\text{Cu}^{\text{I}}\text{--NO}$  and  $\text{NO}^+$ ) and only half of the amount of NO adsorbs to  $\text{Cu}^{\text{II}}$  compared to sites B and C. Additionally we assume that possible close lying  $\text{NO}^+$  species<sup>[13]</sup> do not influence the spectra. Under these assumptions it is now possible to construct the spectrum shown in Figure 4b.

At low NO pressure the occupation of site C leads to a comparatively broad peak with a maximum around  $1840\text{ cm}^{-1}$ . When the pressure increases, site A is occupied

and two clearly defined additional peaks start to appear. The occupation of site B leads to a far more complex spectrum. The highest energy peak shifts slightly and the spectrum of site A soon becomes dominant. This spectrum is red-shifted by about  $40\text{ cm}^{-1}$  compared to experimental measurements, which is well established and can be seen as shortcoming of the applied level of theory.<sup>[16]</sup> Qualitatively we find more minor side peaks in the predicted spectrum, but the main features are in excellent qualitative agreement with the experimental measurements discussed above justifying the assumptions made in the construction of this spectrum.

Owing to a presumed autoreduction of  $\text{Cu}^{\text{II}}$  sites,<sup>[27]</sup> it is difficult to obtain conclusive evidence for the actual distribution of Al sites in the system. Studying the  $\text{Cu}^{\text{II}}\text{--NO}$  peak indicates that at least 1 % of all possible exchange sites correspond to site A, and at least another 4 % to site B. In previous work, site A2 has been identified as the most stable  $\text{Cu}^{\text{II}}$  position in SSZ-13, directly followed by site B.<sup>[11]</sup> It can furthermore be assumed that site C is created by splitting of water over

Cu sites. When assuming that this effect and autoreduction are similar for both sites, the amount of site A is a good estimate for the amount of possible exchange sites. However, it is not possible to draw conclusions about the amount of site B, since it is the least stable site and its amount will increase with increased exchange level.

Interestingly significant catalytic activity in the relevant temperature range of  $200\text{--}300^\circ\text{C}$  only starts to appear for Cu/Al ratios higher than 0.016.<sup>[10]</sup> Combining this observation with the results obtained in this work strongly suggests that sites A and C are catalytically inactive. However, site B seems to be catalytically active for the studied catalyst. This refines previous reports, which suggested that sites A and B are both catalytically active.<sup>[11,12]</sup>

In summary, we modeled the IR spectrum of NO adsorbed to  $\text{Cu}^{\text{II}}$  sites in the zeolite SSZ-13 using molecular dynamics simulations. We show that many of the investigated sites lead to a complex multi-peak spectrum for one NO molecule adsorbed to one active site, which cannot be expected from static calculations. This is caused by two effects, namely the thermal motion of the Cu cation, and a change in the bonding mode of NO to the sites. Comparing the modeled spectra to experimental measurements at low ion exchange levels allows to propose a plausible Cu site distribution and with it a limited part of the Al distribution in

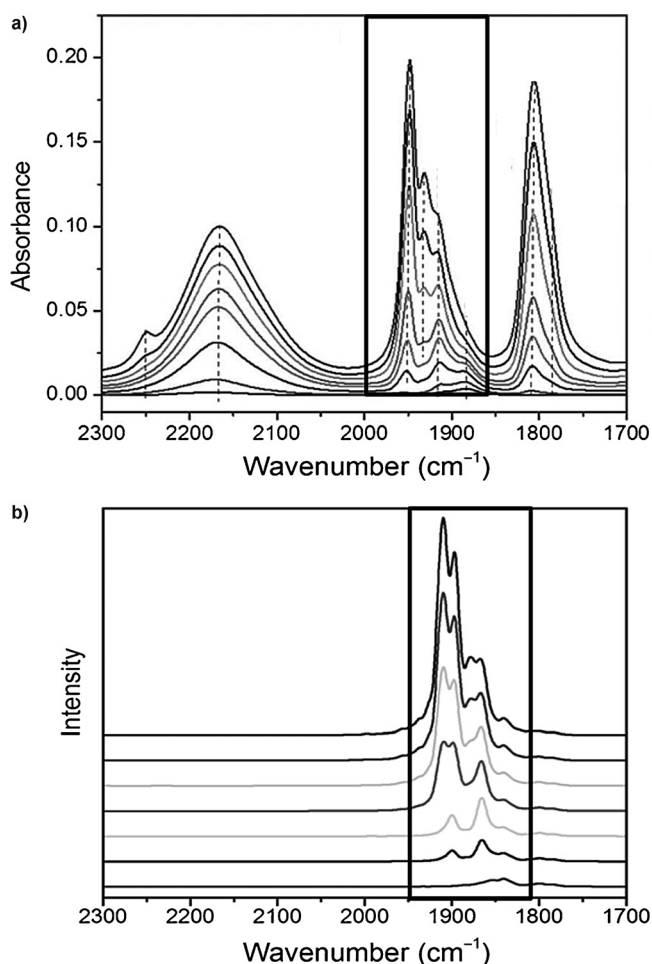


**Figure 4.** a) Experimental and b) simulated IR spectrum for different NO loadings. The investigated Cu<sup>II</sup> feature is highlighted. The modeled spectrum is based upon the assumption of 16.66% of the total site being site C, 16.66% site A, and 66.66% site B. This spectrum is in excellent agreement with experimental data previously reported for Cu-SSZ-13 with a Si/Al ratio of 6 and Cu/Al of 0.03. (a) is adapted with permission from Ref. [13]. Copyright 2014 American Chemical Society.

the framework. Knowing this distribution is one of the key features in arriving at structure–activity relationships for the catalyst at hand. This work clearly shows that it is necessary to use dynamic calculations to understand and assign experimental spectra, since at least for this system, static calculations are not able to reproduce the observed behavior. We expect similar effects to be important in a large number of systems, where the characterized active site is within a shallow minimum of the potential energy surface and can change its coordination regularly.

## Methods

In this work, we performed ab initio molecular dynamics simulations using the Vienna ab initio simulation package (VASP),<sup>[19,20]</sup> a plane wave code using periodic boundary conditions and PAW pseudo potentials.<sup>[28]</sup> The energy cut-off in our calculations was set to 417 eV and only the  $\Gamma$ -point was used. As discussed in the text, we studied 11 different sites and sampled a trajectory of 75 ps using a timestep of

0.5 fs under stochastic boundary conditions<sup>[22]</sup> with a Langevin thermostat. To avoid problems with calculating dipole moments of a rhombohedral unit cell in periodic boundary conditions, we calculated the spectra as Fourier transformations of the distance autocorrelation function.<sup>[29]</sup> In post-processing we furthermore applied a Gaussian smearing (width of 4 cm<sup>-1</sup>) to create spectra comparable to experimental measurements.

**Keywords:** copper zeolites · heterogeneous catalysis · IR spectroscopy · molecular dynamics · SSZ-13

**How to cite:** *Angew. Chem. Int. Ed.* **2015**, 54, 7799–7804  
*Angew. Chem.* **2015**, 127, 7910–7915

- [1] M. Iwamoto, H. Yahiro, Y. Mine, S. Kagawa, *Chem. Lett.* **1989**, 213–216.
- [2] M. Iwamoto, H. Yahiro, K. Tanda, N. Mizuno, Y. Mine, S. Kagawa, *J. Phys. Chem.* **1991**, 95, 3727–3730.
- [3] U. Deka, I. Lezcano-Gonzalez, B. M. Weckhuysen, A. M. Beale, *ACS Catal.* **2013**, 3, 413–427.
- [4] J.-H. Kwak, R. G. Tonkyn, D.-H. Kim, J. Szanyi, H. F. Peden, *J. Catal.* **2010**, 275, 187–190.
- [5] I. Bull, W. M. Xue, P. Burk, R. S. Boorse, W. M. Jaglowski, G. S. Kroemer, A. Moini, J. A. Patchett, J. C. Dettling, M. T. Caudle, U.S. Patent 7 601 662 B2, **2009** to BASF.
- [6] D. W. Fickel, R. Lobo, *J. Phys. Chem. C* **2010**, 114, 1633–1640.
- [7] U. Deka, A. Juhin, E. A. Eilertsen, H. Emerich, M. A. Green, S. T. Korhonen, B. M. Weckhuysen, A. M. Beale, *J. Phys. Chem. C* **2012**, 116, 4809–4818.
- [8] J. H. Kwak, J. H. Lee, S. D. Burton, A. S. Lipton, C. H. F. Peden, J. Szanyi, *Angew. Chem. Int. Ed.* **2013**, 52, 9985–9989; *Angew. Chem.* **2013**, 125, 10169–10173.
- [9] C. Paolucci, A. A. Verma, S. A. Bates, V. F. Kispersky, J. T. Miller, R. Gounder, W. N. Delgass, F. H. Ribeiro, W. F. Schneider, *Angew. Chem. Int. Ed.* **2014**, 53, 11828–11833; *Angew. Chem.* **2014**, 126, 12022–12027.
- [10] F. Gao, E. D. Walter, M. Kollar, Y. Wang, J. Szanyi, C. H. F. Peden, *J. Catal.* **2014**, 319, 1–14.
- [11] F. Göttl, R. E. Bulo, J. Hafner, P. Sautet, *J. Phys. Chem. Lett.* **2013**, 4, 2244–2249.
- [12] S. A. Bates, A. A. Verma, C. Paolucci, A. A. Parekh, T. Anggara, A. Yezerets, W. F. Schneider, J. T. Miller, W. N. Delgass, F. H. Ribeiro, *J. Catal.* **2014**, 312, 87–97.
- [13] R. Zhang, J.-S. McEwen, M. Kollar, F. Gao, Y. Wang, J. Szanyi, C. H. F. Peden, *ACS Catal.* **2014**, 4, 4093–4105.
- [14] S. A. Bates, W. N. Delgass, F. H. Ribeiro, J. T. Miller, R. Gounder, *J. Catal.* **2014**, 312, 26–36.
- [15] A. Godiksen, F. N. Stappen, P. N. R. Vennestrøm, F. Giordanino, S. B. Rasmussen, L. F. Lundegaard, S. Mossin, *J. Phys. Chem. C* **2014**, 118, 23126–23138.
- [16] F. Göttl, J. Hafner, *J. Chem. Phys.* **2012**, 136, 064503.
- [17] F. Göttl, J. Hafner, *J. Chem. Phys.* **2012**, 136, 064501.
- [18] C. W. Andersen, M. Bremholm, P. N. R. Vennestrøm, A. B. Blichfeld, L. F. Lundegaard, B. B. Iversen, *IUCrJ* **2014**, 1, 382–386.
- [19] G. Kresse, J. Hafner, *Phys. Rev. B* **1993**, 48, 13115.
- [20] G. Kresse, J. Furthmüller, *Comput. Mater. Sci.* **1996**, 6, 15.
- [21] M.-P. Gaigeot, *Phys. Chem. Chem. Phys.* **2010**, 12, 3336–3359.
- [22] L. Kantorovich, N. Rompotis, *Phys. Rev. B* **2008**, 78, 094305.
- [23] For the sake of simplicity in the discussion, we will only address the major features. For details, see the Supporting Information.
- [24] T. Janssens, H. Falsig, L. Lundegaard, P. Vennestrøm, S. Rasmussen, P. Moses, F. Giordanino, E. Borfecchia, K. Lomachenko, C. Lamberti, S. Bordiga, A. Godiksen, S. Mossin, P. Beato, *ACS Catal.* **2015**, 5, 2832–2845.

- [25] Site A1 shows very similar results with numerical values of 0.63/0.37 for the spectral analysis compared to 0.56/0.44 from the trajectory analysis.
- [26] In the light of this study, this assignment is not entirely unambiguous, because NO bound to a Cu–OH site in the six-membered ring leads to a very similar IR signal.
- [27] E. Borfecchia, L. A. Lomachenko, F. Giordanino, H. Falsig, P. Beato, A. V. Aldatov, S. Bordiga, C. Lamberti, *Chem. Sci.* **2015**, 6, 548–563.
- [28] P. E. Blöchl, *Phys. Rev. B* **1994**, 50, 17953.
- [29] P. Fleurat-Lassard, C. Michel, R. E. Bulo, *J. Chem. Phys.* **2012**, 137, 074111.

Received: March 1, 2015  
Published online: May 12, 2015